

Supplement of

**Evolution and chemical characteristics of organic aerosols during
wintertime PM_{2.5} episodes in Shanghai, China: Insights gained from
online measurements of organic molecular markers**

Shuhui Zhu et al.

Correspondence to: Jian Zhen Yu (jian.yu@ust.hk) and Cheng Huang (huangc@saes.sh.cn)

Contents of this file:

Text S1 to S2

Table S1 to S2

Figures S1 to S12

References

Table S1. Statistics of hourly concentrations of 98 organic molecules measured by TAG system.

| Group | Compounds | Abbreviation | Avg ng/m ³ | Range ng/m ³ | Internal standards | Quantification ions | Potential sources |
|---------------|---|--------------|--------------------------|----------------------------|---------------------|------------------------|---|
| L_DCAs | Malonic acid | C3 | 0.66 | 0.04-5.54 | Adipic acid-d10 | 233 | Oxidation products of VOCs |
| | Succinic acid | C4 | 77.8 | 3.50-498.4 | Succinic acid-d4 | 247 | |
| | Glutaric acid | C5 | 16.1 | 0.73-150.6 | | 261 | |
| L_hDCAs | Malic_acid | hC4 | 155.5 | 10.1-568.1 | Azelaic Acid-d14 | 233 | Oxidation products of VOCs |
| | Citramalic_acid | hiC5 | 29.4 | 2.16-142.1 | | 247 | |
| | Glyceric_acid | hC3 | 53.5 | 3.33-234.5 | Succinic acid-d4 | 292 | |
| | 2-hydroxyglutaric acid | 2-hC5 | 2.26 | 0.04-13.7 | Adipic acid-d10 | 349 | |
| | 3-hydroxyglutaric acid | 3-hC5 | 23.7 | 0.70-170.6 | | 349 | |
| H_DCAs | Adipic acid | C6 | 9.54 | 0.71-64.4 | Adipic acid-d10 | 111 | Oxidation products of VOCs |
| | Pimelic acid | C7 | 2.22 | 0.17-15.5 | Azelaic Acid-d14 | 289 | |
| | Suberic acid | C8 | 4.05 | 0.08-26.6 | | 303 | |
| H_hDCAs | 2-hydroxyadipic acid | 2-hC6 | 3.06 | 0.05-22.9 | Adipic acid-d10 | 363 | Oxidation products of VOCs |
| | 3-Hydroxyadipic acid | 3-hC6 | 15.4 | 0.40-116.4 | | 363 | |
| | Hydroxypimelic acid | hC7 | 6.95 | 0.30-39.4 | Azelaic Acid-d14 | 377 | |
| α PinT | Pinic acid | PA | 7.55 | 0.38-34.3 | Azelaic Acid-d14 | 171 | Oxidation products of α - pinene |
| | Pinonic acid | PNA | 1.03 | 0.09-6.47 | | 171 | |
| | 3-methyl-1,2,3-butanetricarboxylic acid | 3-MBTCA | 4.34 | 0.10-26.0 | | 405 | |
| | 3-acetylglutaric acid | 3-AGA | 3.73 | 0.40-15.1 | | 303 | |
| | 3-hydroxy-4,4-dimethylglutaric | 3-HDGA | 12.6 | 0.06-67.3 | | 377 | |
| β CaryT | β -caryophyllinic acid | b-CA | 1.36 | BD-5.15 | Azelaic Acid-d14 | 383 | Oxidation product of β - caryophyllene |
| DHOPA | 2,3-dihydroxy-4-oxopentanoic acid | DHOPA | 12.9 | 0.47-58.6 | Azelaic Acid-d14 | 277 | Oxidation product of mono- aromatics |
| Pht | Phthalic acid | Pht | 28.8 | 1.28-147.1 | Phthalic-3,4,5,6-d4 | 295 | Oxidation product of |

| | | | | | acid | | naphthalene and derivatives |
|---|--------------------------------|---------|------|------------|---------------------|-----|--|
| Aromatic polycarboxylic acids (Ar-PCAs) | Isophthalic acid | iPh | 1.75 | 0.12-9.14 | | 295 | |
| | Terephthalic acid | tPh | 21.1 | 0.94-105.3 | Phthalic-3,4,5,6-d4 | 295 | Oxidation products of aromatic compounds |
| | 1,2,4-benzentricarboxylic acid | 124BTCA | 15.1 | 0.25-98.4 | acid | 411 | |
| | 1,3,5-benzentricarboxylic acid | 135BTCA | 2.49 | 0.16-15.1 | | 411 | |
| Nitro-aromatic compounds (NACs) | 4-nitrocatechol | 4NC | 1.54 | BD-9.42 | | 284 | |
| | 4-nitrophenol | 4NP | 3.33 | 0.06-20.7 | Phthalic-3,4,5,6-d4 | 196 | Nitration of aromatic compounds |
| | 3-methyl-5-nitrocatechol | 3M5NC | 0.24 | BD-1.30 | acid | 298 | |
| | 4-methyl-5-nitrocatechol | 4M5NC | 0.66 | BD-4.00 | | 298 | |
| Biomass burning tracers (BBtracers) | 3-hydroxybenzoic acid | 3-HBA | 0.76 | 0.05-3.36 | | 267 | |
| | 4-hydroxybenzoic acid | 4-HBA | 1.40 | 0.09-6.41 | Phthalic-3,4,5,6-d4 | 267 | |
| | Syringic acid | SyrinA | 0.65 | 0.02-3.97 | acid | 327 | |
| | Vanillic acid | VaniA | 0.57 | 0.03-3.27 | | 267 | Biomass burning |
| | Galactosan | Gal | 2.44 | 0.13-12.8 | | 217 | |
| | Mannosan | Manno | 4.54 | 0.36-19.4 | Levogluconan-d7 | 204 | |
| | Levogluconan | Levo | 61.3 | 5.18-185.1 | | 204 | |
| Primary sugars | Mannitol | Manni | 31.3 | 1.92-155.0 | | 319 | Plant debris, fungal spores |
| | Glucose | Glu | 5.17 | 0.51-21.8 | Glucose-d7 | 204 | |
| C9 acids | Azeleic_acid | C9 | 10.5 | 1.02-62.1 | | 317 | Oxidation products of long-chain fatty acids |
| | 9-oxononanoic acid | ωC9:0 | 5.95 | 0.45-36.4 | Azelaic Acid-d14 | 228 | |
| | Nonanoic acid | C9:0 | 0.58 | 0.04-5.05 | | 215 | |
| Saturated fatty acids (sFAs) | Decanoic acid | C10:0 | 2.00 | 0.14-12.6 | Azelaic Acid-d14 | 229 | |
| | Undecanoic acid | C11:0 | 0.06 | BD-0.32 | | 243 | |
| | Lauric acid | C12:0 | 0.86 | 0.05-6.26 | | 257 | |
| | Tridecanoic acid | C13:0 | 0.11 | 0.02-0.58 | Myristic acid-d27 | 271 | Cooking |
| | Myristic acid | C14:0 | 2.92 | 0.18-21.6 | | 285 | |
| | Pentadecanoic acid | C15:0 | 0.85 | 0.10-5.88 | | 299 | |
| | Palmitic acid | C16:0 | 53.9 | 4.39-360.8 | Palmitic acid-d31 | 313 | |

| | | | | | | | |
|--------------------------------|-------------------------------|---------------------|------|------------|--------------------|-----|-----------------------------|
| | Heptadecanoic acid | C17:0 | 0.93 | 0.05-9.98 | | 327 | |
| | Stearic acid | C18:0 | 30.2 | 2.20-283.0 | | 341 | |
| | Nonadecanoic acid | C19:0 | 0.34 | 0.03-3.68 | Stearic acid-d35 | 355 | |
| | Eicosanoic acid | C20:0 | 0.84 | 0.04-10.1 | | 369 | |
| Unsaturated fatty acids (uFAs) | Oleic acid | C18:1 | 20.5 | 0.64-178.2 | Stearic acid-d35 | 339 | |
| | Palmitoleic acid | C16:1 | 0.36 | 0.03-3.31 | Palmitic acid-d31 | 311 | Cooking |
| | Linoleic acid | C18:2 | 7.76 | 0.07-164.6 | Stearic acid-d35 | 337 | |
| Alkanes | Heneicosane | n-C21 | 0.99 | 0.20-5.35 | n-Eicosane-d42 | 57 | |
| | Docosane | n-C22 | 1.94 | 0.29-9.29 | | 57 | |
| | Tricosane | n-C23 | 1.95 | 0.25-11.6 | | 57 | |
| | Tetracosane | n-C24 | 3.05 | 0.43-13.5 | n-Tetracosane-d50 | 57 | |
| | Pentacosane | n-C25 | 4.73 | 0.67-25.6 | | 57 | |
| | Hexacosane | n-C26 | 4.12 | 0.48-22.0 | | 57 | |
| | Heptacosane | n-C27 | 4.65 | 0.52-25.8 | | 57 | |
| | Octacosane | n-C28 | 3.41 | 0.26-22.3 | | 57 | |
| | Nonacosane | n-C29 | 4.36 | 0.29-23.9 | | 57 | Vegetative detritus, fossil |
| | Tracotane | n-C30 | 2.38 | 0.02-17.2 | n-Octacosane-d58 | 57 | fuel uses |
| | Hentriacontane | n-C31 | 2.01 | 0.02-12.5 | | 57 | |
| | Dotriacontane | n-C32 | 1.39 | 0.02-13.4 | | 57 | |
| | Tritactotane | n-C33 | 0.73 | BD-5.67 | | 57 | |
| | Tetratriacontane | n-C34 | 0.60 | 0.02-4.37 | | 57 | |
| | Pentatriacontane | n-C35 | 0.56 | BD-4.39 | n-Hexatriacontane- | 57 | |
| | Hexatriacontane | n-C36 | 0.38 | BD-2.91 | d74 | 57 | |
| | Heptatriacontane | n-C37 | 0.22 | BD-2.36 | | 57 | |
| Hopanes | 22,29,30-trisnorhopane | C27Tm | 0.04 | BD-0.26 | | 191 | |
| | $\alpha\beta$ -norhopane | C29 $\alpha\beta$ | 0.37 | 0.03-1.96 | n-Tetracosane-d50 | 191 | Vehicular emission, coal |
| | $\alpha\beta$ -hopane | C30 $\alpha\beta$ | 0.46 | BD-2.32 | | 191 | combustion |
| | $\alpha\beta$ -22S-homohopane | C31 $\alpha\beta$ S | 0.11 | BD-0.66 | | 191 | |

| | | | | | | | |
|------|-------------------------------|---------------------|------|-----------|--------------------|-----|---|
| | $\alpha\beta$ -22R-homohopane | C31 $\alpha\beta$ R | 0.11 | BD-0.70 | | 191 | |
| PAHs | Phenanthrene | Phe | 0.43 | 0.07-1.34 | | 178 | |
| | Anthracene | Ant | 0.18 | 0.01-0.54 | | 178 | |
| | Fluoranthene | Flu | 0.41 | 0.03-3.38 | | 202 | |
| | Pyrene | Pyr | 0.38 | BD-3.48 | | 202 | |
| | Benzo[b]chrysene | BbC | 0.02 | BD-0.31 | Phenanthrene-d10 | 278 | |
| | Benzo[c]phenanthrene | BcP | 0.05 | BD-0.40 | | 228 | |
| | Cyclopenta[cd]pyrene | CcdP | 0.07 | BD-0.86 | | 226 | |
| | Dibena[a,c]anthracene | DacA | 0.02 | BD-0.42 | | 278 | |
| | Triphenylene | TriP | 0.18 | BD-2.39 | | 228 | |
| | Chrysene | Chr | 0.22 | 0.02-1.26 | Chrysene-d12 | 228 | Combustion sources (e.g., coal combustion) |
| | Benzo[a]anthracene | BaA | 0.17 | BD-1.46 | | 228 | |
| | Benzo[b]fluoranthene | BbF | 0.23 | 0.01-1.48 | | 252 | |
| | Benzo[k]fluoranthene | BkF | 0.43 | BD-2.69 | | 252 | |
| | Benzo[a]fluoranthene | BaF | 0.12 | BD-1.14 | Perylene-d12 | 252 | |
| | Benzo[e]pyrene | BeP | 0.42 | 0.03-2.49 | | 252 | |
| | Benzo[a]pyrene | BaP | 0.45 | BD-3.85 | | 252 | |
| | Perylene | Per | 0.18 | BD-1.81 | | 252 | |
| | Indeno[1,2,3-cd]pyrene | IcdP | 0.38 | BD-3.15 | Benzo[ghi]perylene | 276 | |
| | Benzo[ghi]perylene | BghiP | 0.53 | 0.04-2.47 | -d12 | 276 | |
| | Dibenzo[a,h]anthracene | DahA | 0.09 | BD-1.08 | | 278 | |

Table S2. Statistics of hourly concentrations of all VOC species measured by GC-FID and their corresponding subgroups.

| Subgroups | Species | Avg ppb | Range ppb |
|-----------|------------------------|------------|--------------|
| Alkanes | Ethane | 6.91 | 0.22-33.6 |
| | Propane | 5.47 | 0.16-51.6 |
| | Isobutane | 1.39 | 0.06-10.2 |
| | n-Butane | 1.82 | 0.09-18.8 |
| | Cyclopentane | 0.10 | BD-1.20 |
| | Isopentane | 0.87 | 0.06-6.19 |
| | n-Pentane | 0.60 | 0.01-3.15 |
| | 2,2-Dimethylbutane | 0.04 | BD-0.97 |
| | 2,3-Dimethylbutane | 0.07 | BD-0.97 |
| | 2-Methylpentane | 0.18 | BD-1.18 |
| | 3-Methylpentane | 0.18 | BD-1.00 |
| | n-Hexane | 0.30 | 0.02-2.00 |
| | 2,4-Dimethylpentane | 0.03 | BD-1.04 |
| | Methylcyclopentane | 0.09 | BD-0.98 |
| | 2-Methylhexane | 0.08 | BD-1.01 |
| | Cyclohexane | 0.15 | BD-1.51 |
| | 2,3-Dimethylpentane | 0.03 | BD-1.01 |
| | 3-Methylhexane | 0.08 | BD-1.79 |
| | 2,2,4-Trimethylpentane | 0.05 | BD-1.01 |
| | n-Heptane | 0.13 | BD-3.09 |
| | Methylcyclohexane | 0.09 | BD-1.01 |
| | 2,3,4-Trimethylpentane | 0.04 | BD-1.03 |
| | 2-Methylheptane | 0.03 | BD-1.05 |
| | 3-Methylheptane | 0.03 | BD-1.06 |
| | n-Octane | 0.10 | 0.01-3.46 |
| | n-Nonane | 0.18 | 0.01-3.88 |
| | n-Decane | 0.08 | 0.01-1.08 |
| Alkenes | Ethylene | 2.49 | 0.04-27.0 |
| | Propylene | 0.63 | BD-11.9 |
| | Trans-2-butene | 0.08 | BD-1.38 |
| | 1-Butene | 0.12 | BD-1.10 |
| | Isobutylene | 0.14 | 0.02-0.53 |
| | cis-2-Butene | 0.06 | BD-1.10 |
| | 1,3-Butadiene | 0.03 | BD-0.40 |
| | 1-Pentene | 0.03 | BD-1.19 |
| | trans-2-Pentene | 0.03 | BD-1.19 |
| | Isoprene | 0.04 | BD-1.10 |
| | cis-2-Pentene | 0.02 | BD-1.15 |
| | 1-Hexene | 0.02 | BD-0.96 |
| | 3-Methyl-1-butene | 0.01 | BD-0.06 |

| | | | |
|-----------|-------------------------|-------|-----------|
| | 2-Methyl-1-butene | 0.02 | BD-0.11 |
| | 2-Methyl-2-butene | 0.01 | BD-0.23 |
| | 4-Methyl-1-pentene | 0.002 | BD-0.02 |
| | 2-Methyl-1-pentene | 0.02 | BD-0.47 |
| | 2-Methyl-2-pentene | 0.001 | BD-0.02 |
| Acetylene | Acetylene | 2.08 | 0.02-19.3 |
| Aromatics | Benzene | 0.59 | 0.04-1.94 |
| | Toluene | 1.21 | 0.06-7.35 |
| | Ethylbenzene | 0.38 | 0.02-5.39 |
| | m/p-Xylene | 0.70 | BD-10.8 |
| | o-Xylene | 0.32 | 0.02-3.54 |
| | Styrene | 0.09 | BD-0.95 |
| | iso-Propylbenzene | 0.03 | BD-1.03 |
| | n-Propylbenzene | 0.05 | BD-1.01 |
| | m-Ethyltoluene | 0.06 | BD-1.10 |
| | p-Ethyltoluene | 0.05 | BD-1.06 |
| | 1,3,5-Trimethylbenzene | 0.05 | BD-1.05 |
| | o-Ethyltoluene | 0.05 | BD-1.01 |
| | 1,2,4-Trimethylbenzene | 0.07 | BD-0.91 |
| | 1,2,3-Trimethylbenzene | 0.06 | BD-1.00 |
| | m-Diethylbenzene | 0.04 | BD-1.02 |
| | p-Diethylbenzene | 0.05 | BD-0.92 |
| OVOCs | Acetaldehyde | 0.84 | 0.08-5.36 |
| | Acrolein | 0.10 | BD-0.51 |
| | Propanal | 0.23 | 0.05-1.05 |
| | n-Butanal | 0.09 | 0.01-0.56 |
| | Methacrolein | 0.02 | BD-0.14 |
| | Methylvinylketone | 0.03 | BD-0.20 |
| | Methylethylketone | 0.80 | 0.02-6.87 |
| | 2-Pentanone | 0.02 | BD-0.13 |
| | n-Pentanal | 0.06 | BD-0.36 |
| | 3-Pentanone | 0.02 | BD-0.07 |
| | Methyl isobutyl ketone | 0.04 | BD-0.38 |
| | n-Hexanal | 0.16 | 0.01-1.85 |
| | Methyl tert-butyl ether | 0.15 | BD-1.86 |
| | Isopropyl alcohol | 0.39 | 0.03-10.9 |
| | Methyl acetate | 0.53 | 0.01-16.2 |
| | Ethyl acetate | 0.95 | 0.01-15.1 |
| | n-Propyl acetate | 0.18 | BD-7.44 |
| | n-Butyl acetate | 0.37 | 0.01-2.98 |
| | Methyl methacrylate | 0.01 | BD-0.14 |
| | Vinyl acetate | 0.01 | BD-0.28 |
| | Acetonitrile | 0.53 | 0.05-19.3 |
| XVOCs | Freon-114 | 0.01 | BD-0.04 |

| | | |
|---------------------------|-------|-----------|
| Chloromethane | 0.17 | 0.01-0.89 |
| Vinylchloride | 0.01 | BD-0.13 |
| Bromomethane | 0.01 | BD-0.16 |
| Chloroethane | 0.04 | BD-2.06 |
| Freon-11 | 0.62 | 0.01-22.1 |
| 1,1-Dichloroethene | 0.003 | BD-0.07 |
| Freon-113 | 0.06 | BD-0.21 |
| Dichloromethane | 1.58 | 0.05-14.6 |
| 1,1-Dichloroethane | 0.01 | BD-0.19 |
| cis-1,2-Dichloroethene | 0.003 | BD-0.04 |
| Chloroform | 0.25 | BD-26.1 |
| 1,1,1-Trichloroethane | 0.002 | BD-0.01 |
| Carbontetrachloride | 0.14 | BD-7.65 |
| 1,2-Dichloroethane | 0.54 | 0.01-5.97 |
| Trichloroethylene | 0.07 | BD-2.46 |
| 1,2-Dichloropropane | 0.14 | BD-5.25 |
| Bromodichloromethane | 0.003 | BD-0.01 |
| trans-1,3-Dichloropropene | 0.003 | BD-0.14 |
| cis-1,3-Dichloropropene | 0.003 | BD-0.06 |
| 1,1,2-Trichloroethane | 0.03 | BD-0.32 |
| Tetrachloroethylene | 0.11 | 0.01-8.88 |
| 1,2-Dibromoethane | 0.002 | BD-0.03 |
| Chlorobenzene | 0.03 | BD-0.43 |
| 1,3-Dichlorobenzene | 0.02 | 0.01-0.09 |
| Benzylchloride | 0.03 | 0.01-0.22 |
| 1,2-Dichlorobenzene | 0.03 | 0.01-0.17 |

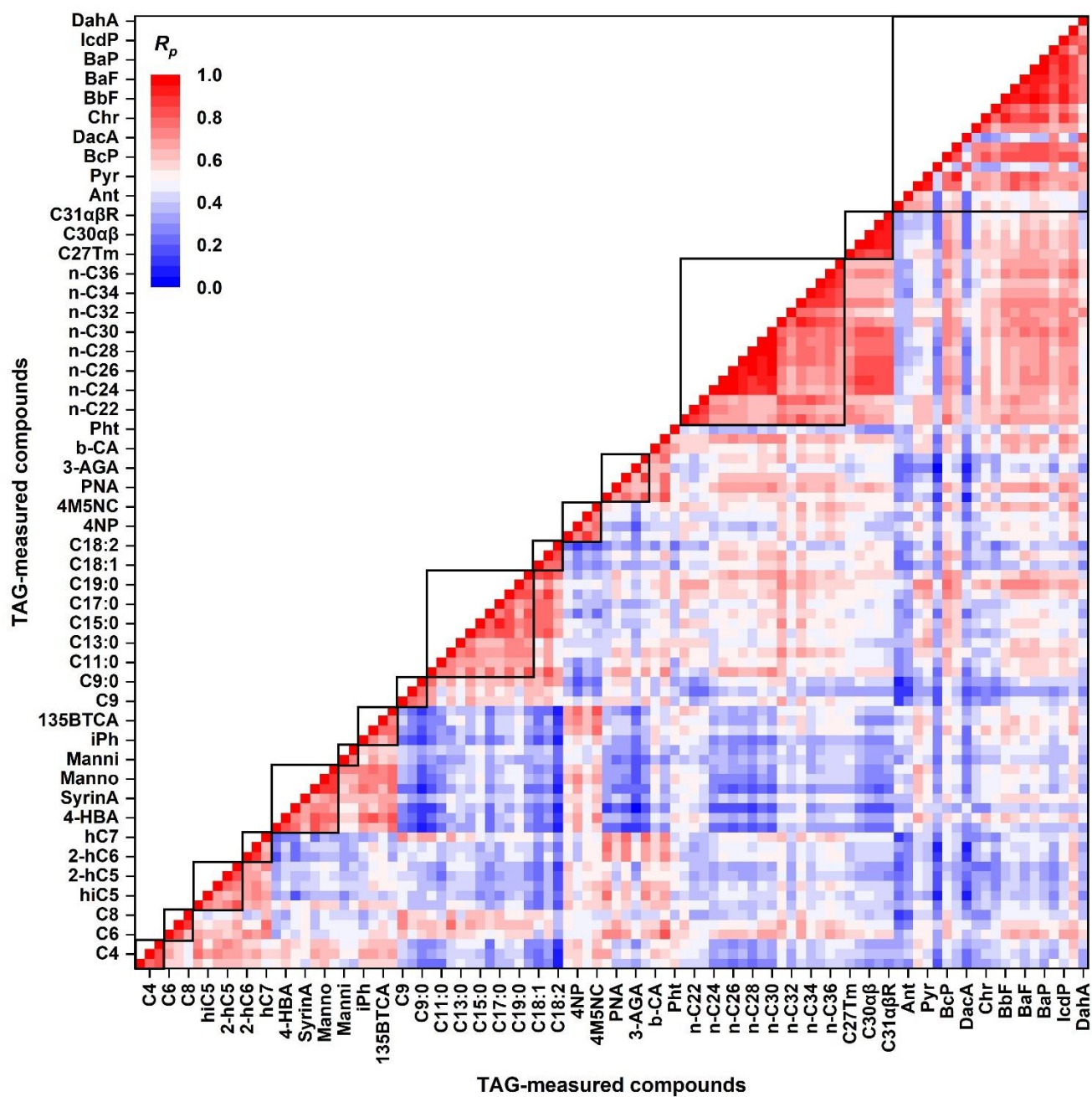


Figure S1. Pearson coefficients (R_p) of hourly concentrations 98 TAG-measured organic molecules. Organic molecules in each dark square box characterized by high R_p are classified into the same organic molecular group. The order of organic molecules is same with Table S2.

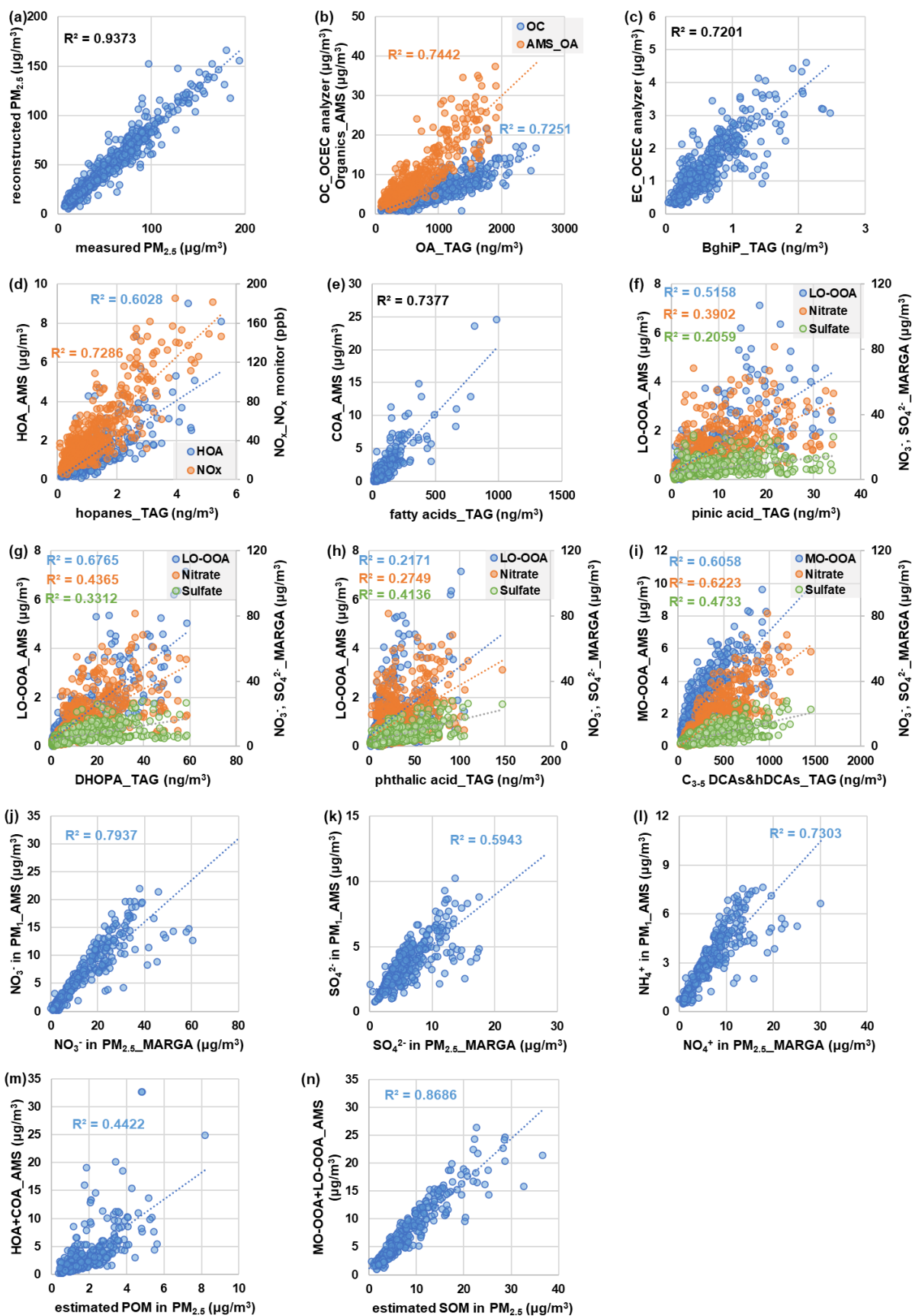


Figure S2. Scatter plots of select pairs of measured parameters with known underlying physical relationships. They serve as internal data consistency check.

30 Text S1. Clustering analysis and concentration weighted trajectory (CWT)

For every hour during the field campaign, a 48-hour backward trajectory starting at 100 m above the observation site was calculated by HYSPLIT software with 6-hour archived GDAS data as meteorological input. Then all the backward trajectories were clustered by calculating their spatial dissimilarity (SPVAR) and total spatial dissimilarity (TSV):

$$SPVAR = \sum_{j=1}^x \sum_{i=1}^t D_{ij}^2 \quad (1)$$

35 where D_{ij} is the distance from the stop point at the j^{th} hour in the i^{th} trajectory to the corresponding point in the average trajectory, t is the length of the trajectory, x is the number of trajectories in the cluster. Then TSV as shown in Figure S3 is calculated by summing up the SPVAR values of all clusters. The variations of PM_{2.5} chemical composition under each cluster is given in Figure S4. Apparently, PM_{2.5} chemical compositions were diverse under different air mass clusters with higher mass fractions of secondary organic matter (SOM) and sulfate observed under cluster 1 (CL#1). In comparison, cluster 2 (CL#2) was
40 characterized by significantly higher mass loading of nitrate, and cluster 3 (CL#3) was characterized by higher mass percentages of elemental carbon (EC) and primary organic matter (POM). For cluster 4 (CL#4), higher mass proportions of sulfate and chloride were observed.

The potential source areas for PM_{2.5} in Shanghai under the influence of different air mass clusters were then analyzed and illustrated by concentration weighted trajectory (CWT) approach with the adoption of ZeFir software based on the results
45 derived from HYSPLIT. With the input of hourly PM_{2.5} concentration data, the residence time of a back trajectory arriving at Shanghai in each $0.2^\circ \times 0.2^\circ$ grid cell of a $25\text{-}50^\circ\text{N} \times 105\text{-}135^\circ\text{E}$ geographical domain is determined via the following equation:

$$CWT_{ij} = \frac{\sum_{L=1}^M C_L \tau_{ij-L}}{\sum_{L=1}^M \tau_{ij-L}} \quad (2)$$

where CWT_{ij} is the attributed PM_{2.5} concentrations in the ij^{th} grid cell, L is the index of the trajectory, M is the total number of back trajectories over a time period, C_L is the hourly concentration of PM_{2.5} corresponding to the arrival of back trajectory L ,
50 τ_{ij-L} is the number of trajectory segment endpoints in the ij^{th} grid cell for back trajectory L .

A weighted function was applied to downweigh cells associated with low values of n_{ij} to lower uncertainties, which was based on the trajectory density by calculating $\log(n+1)$ as described by Bressi et al. (2014) and Waked et al. (2014). The weighted function is empirically determined using the following equations:

$$W = \begin{cases} 1, & \text{for } \log(n+1) > 0.85 * \max_{\log(n+1)} \\ 0.725, & \text{for } 0.6 * \max_{\log(n+1)} < \log(n+1) < 0.85 * \max_{\log(n+1)} \\ 0.475, & \text{for } 0.35 * \max_{\log(n+1)} < \log(n+1) < 0.6 * \max_{\log(n+1)} \\ 0.175, & \text{for } \log(n+1) < 0.35 * \max_{\log(n+1)} \end{cases} \quad (3)$$

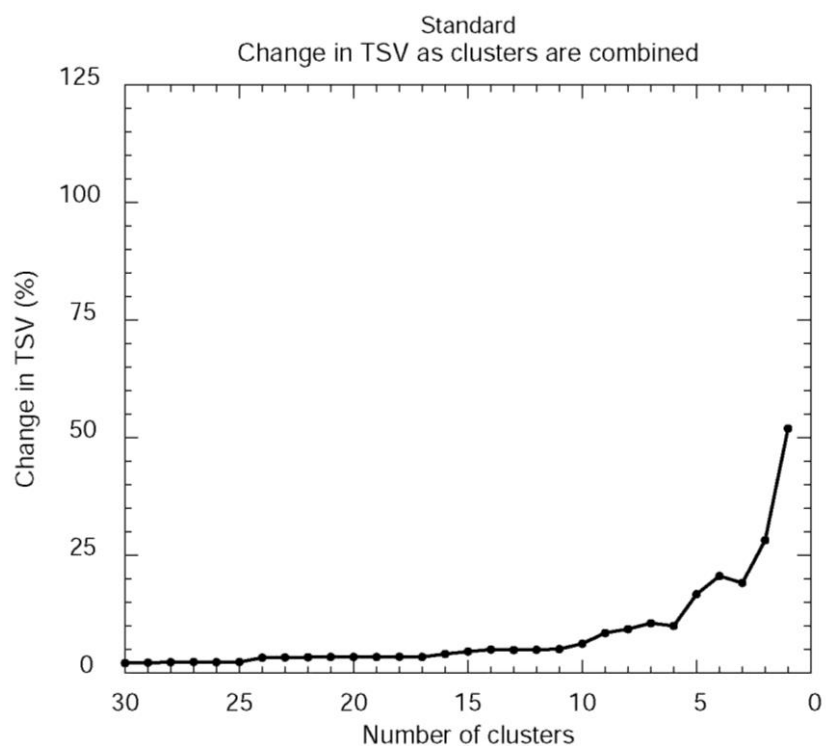


Figure S3. Change of total spatial variance (TSV) as a function of number of clusters for 100m arrival heights.

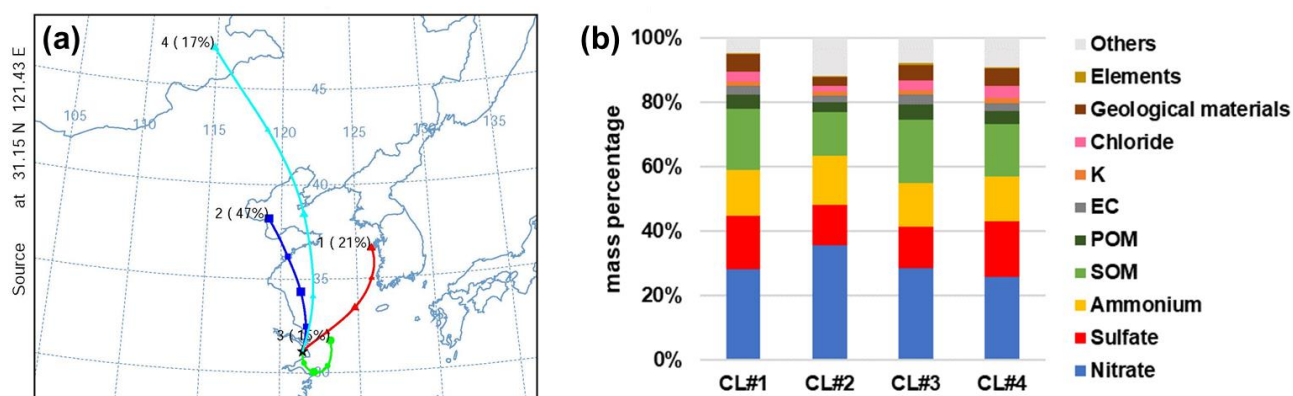


Figure S4. (a) Distribution of the 48-hour backward trajectory clusters arriving at SAES site at 100m above sea level during the campaign; (b) PM_{2.5} chemical compositions under the influences of different clusters

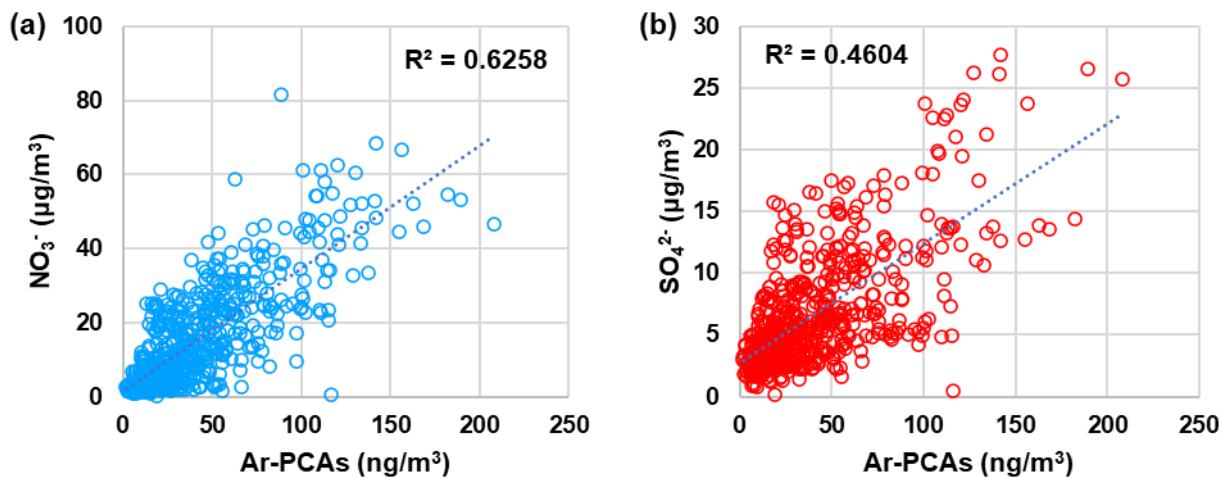
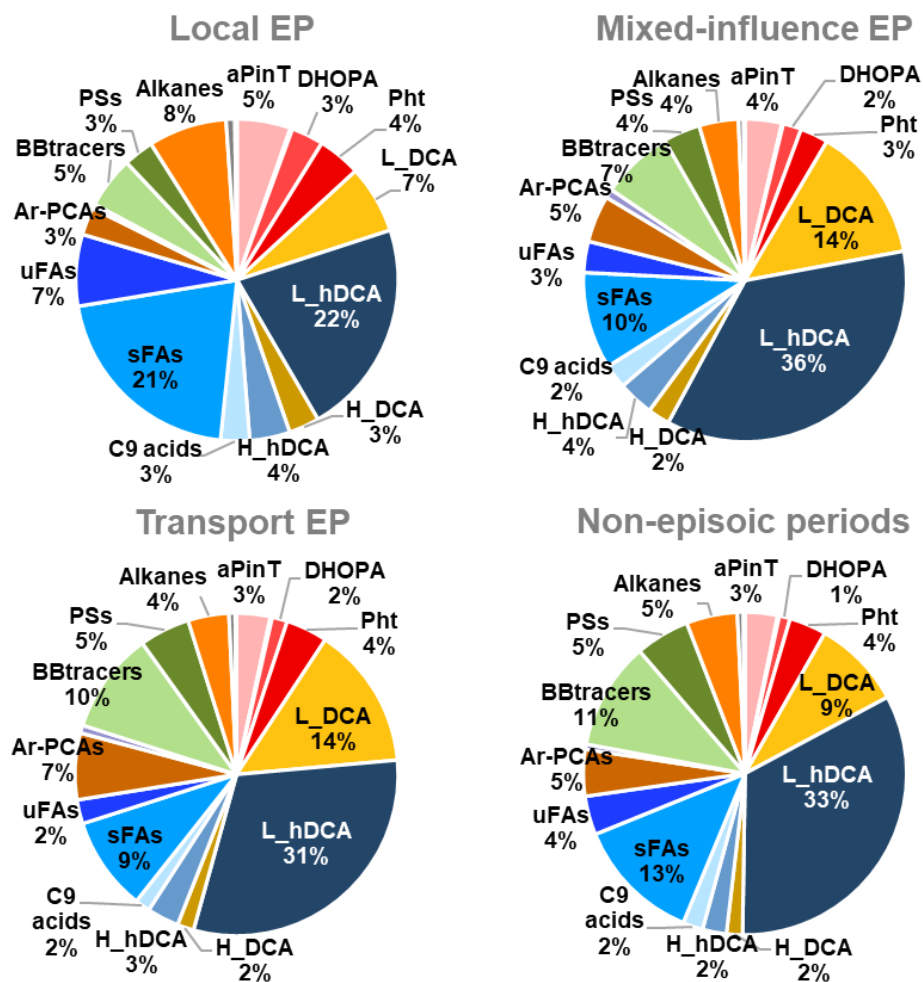


Figure S5. Scatter plots of hourly concentrations of Ar-PCAs versus (a) nitrate and (b) sulfate.



65 Figure S6. Mass proportions of 18-organic molecular groups in TAG-measured OA during the local episodes, mixed-influence episodes, transport episodes, and non-episodic periods, respectively.

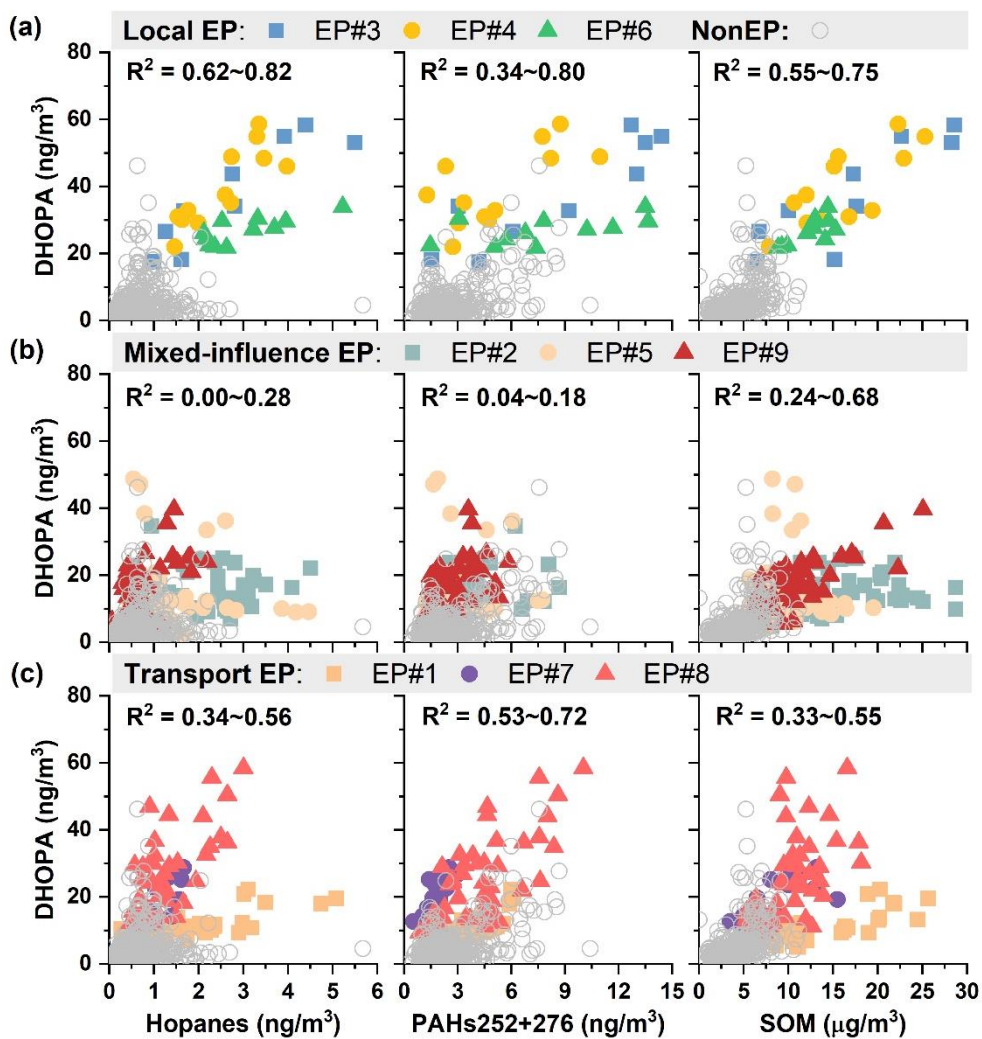


Figure S7. Correlations of DHOPA versus hopanes, PAHs and SOM during (a) local, (b) mixed-influence and (c) transport episodes.

70 PAHs252+276 represents the sum of hourly concentrations of BbF, BkF, BaF, BeP, BaP, IcdP, BghiP measured during the campaign.

TextS2. Estimation of aromatic SOA

A modified tracer-based method for estimating aromatic SOA was proposed in Gao et al. (2019) and Zhang et al. (2021a), which has taken into consideration of equilibrium gas-particle partitioning of semi-volatile products. In this method, the hourly concentration of DHOPA, the oxidation product of monoaromatic compounds, is predicted with the following equations:

$$[DHOPA] = \sum_{i=1}^N \alpha_i \cdot [VOC_{i,consumed}] \quad (4)$$

$$[VOC_{i,consumed}] = VOC_{i,t} \times (\exp(k_i[OH]\Delta t) - 1) \quad (5)$$

$$[OH]\Delta t = \frac{1}{k_x - k_B} \times \left(\ln \frac{[X]}{[B]} \Big|_{t=t_0} - \ln \frac{[X]}{[B]} \Big|_{t=t} \right) \quad (6)$$

where the mass yield values (α_i) of DHOPA from a specific aromatic precursor i were obtained from (Al-Naiema et al., 2020), and k_i is the reaction rate coefficient of precursor i with OH radical. Equations (5) and (6) estimate the VOC precursors consumed (Gouw et al., 2018; Borbon et al., 2013; Yuan et al., 2012; Y. Zhu et al., 2017). Due to the predominant presence of toluene and xylenes in urban area (Al-Naiema et al., 2020; Kleindienst et al., 2007; Zhang et al., 2021a), only include these two aromatic precursors were considered in the calculation. In other words, $[VOC_{i,consumed}]$ in these equations refers to the consumed mass concentrations of toluene and xylenes by OH radicals, and their corresponding α_i values were 0.0019 for toluene and 0.00090 for xylenes under high-NO_x conditions. Note that our monitoring site had an average NO level at 10.4 ± 19.7 ppb (>1 ppb) and VOCs/NO_x ratio at 1.1 ± 0.7 (<10) during the campaign, consistent with the high NO_x conditions created in the chamber studies. $\frac{[X]}{[B]} \Big|_{t=t}$ is the measured ratio of m+p-xylene to benzene at time t . $\frac{[X]}{[B]} \Big|_{t=t_0}$ represents the concentration ratio in fresh emission before aging begins, which is assumed to be constant during the investigation period. The initial emission ratio was determined by conducting a linear fit on a selected dataset of m+p-xylene and benzene ambient concentrations measured in the early morning (0:00-6:00 A.M.) and with ratios of xylenes to benzene fell in the top 10% range. The ratio is calculated to be 3.5 ppb/ppb, which is close to the slope of the upper “edge” in the scatterplot (Figure S8).

The estimated hourly DHOPA values using equations (4)-(6) are in good agreement with ambient measurements as shown in Figure S9, providing confidence that this modified method reasonably describes the formation and partitioning of DHOPA from multiple aromatic hydrocarbon precursors at this site. Subsequently, semi-volatile mono-aromatic SOA (SemiASOA) and total mono-aromatic SOA (TotalASOA), the latter of which includes more-oxidized aromatic SOA (MoASOA) like oligomers and dicarbonyl compounds, are estimated by the following equations proposed by Zhang et al. (2021a). Then MoASOA can be estimated by subtracting SemiASOA from TotalASOA:

$$SemiASOA = \frac{[DHOPA]}{f_{SOA}} \quad (7)$$

$$TotalASOA = \frac{[DHOPA]}{0.0020} \quad (8)$$

$$MoASOA = TotalASOA - SemiASOA \quad (9)$$

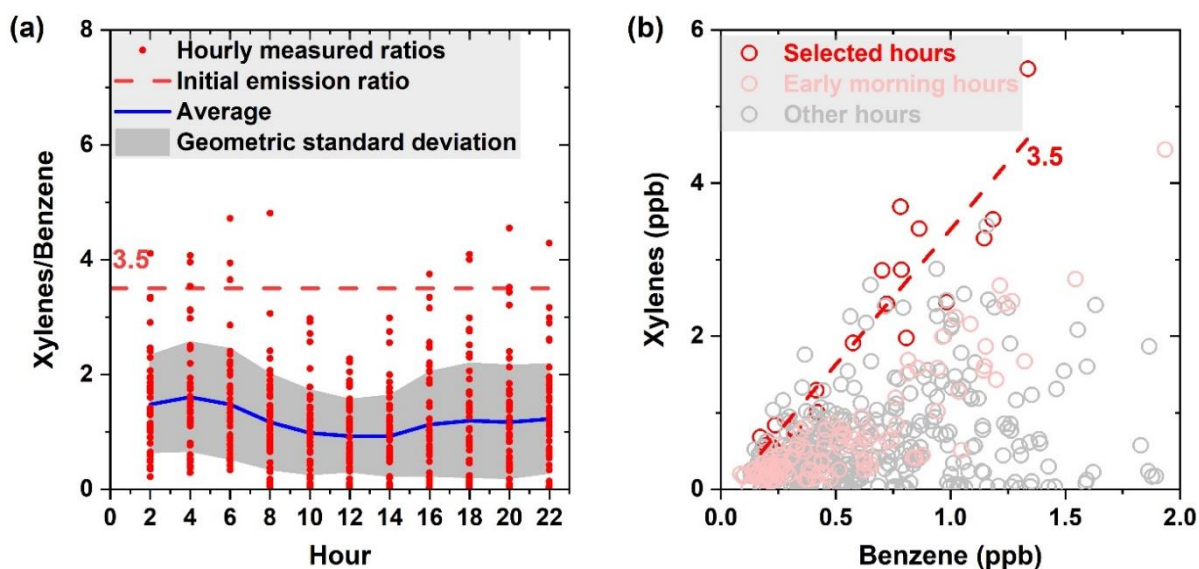
where f_{SOA} is the mass ratio of particle-phase DHOPA to SOA, which can be calculated by equation (10). The mass yield of DHOPA (α) in equation (10) is defined as the ratio of the amount of DHOPA produced to the amount of precursor VOC reacted, and β_i is the mass yield of an individual semi-volatile product i . In this study, α and β_i values for toluene and xylene under high NO_x environment were adopted from Zhang et al. (2021a). $F_{p,t}$ and $F_{p,i}$ are the fraction of DHOPA and semi-volatile products in the absorbing OM phase, respectively, which were estimated using equation (11) and (12), respectively. C_{OA} in the equations

105 represents the mass concentrations of organic aerosols, which were estimated from summing SOM and POM calculated in
 Section 2.2.2. The K_{OM} in equation (11) is the absorptive gas/particle partitioning coefficient of DHOPA and C_i^* in equation
 (12) is the saturation mass concentration of the products oxidized from toluene and xylene, both values of which were also
 adopted from Zhang et al. (2021a).

$$f_{SOA} = \frac{\alpha F_{p,t}}{\sum_{i=1}^N \beta_i F_{p,i}} \quad (10)$$

$$F_{p,t} = \left(1 + \frac{1}{K_{OM} C_{OA}}\right)^{-1} \quad (11)$$

$$F_{p,i} = \left(1 + \frac{C_i^*}{C_{OA}}\right)^{-1} \quad (12)$$



115 **Figure S8.** (a) Diurnal variations of m+p-xylene/benzene concentration ratios during the campaign. Red dots are measured hourly ratios. Blue line indicates hourly geometric average, and gray area represents geometric standard deviations; (b) scatter correlation of m+p-xylene with benzene. Data selected for estimation of initial emission ratio were colored with red. The dashed red line in both graphs show the estimated initial emission ratio of m+p-xylene/benzene which is 3.5.

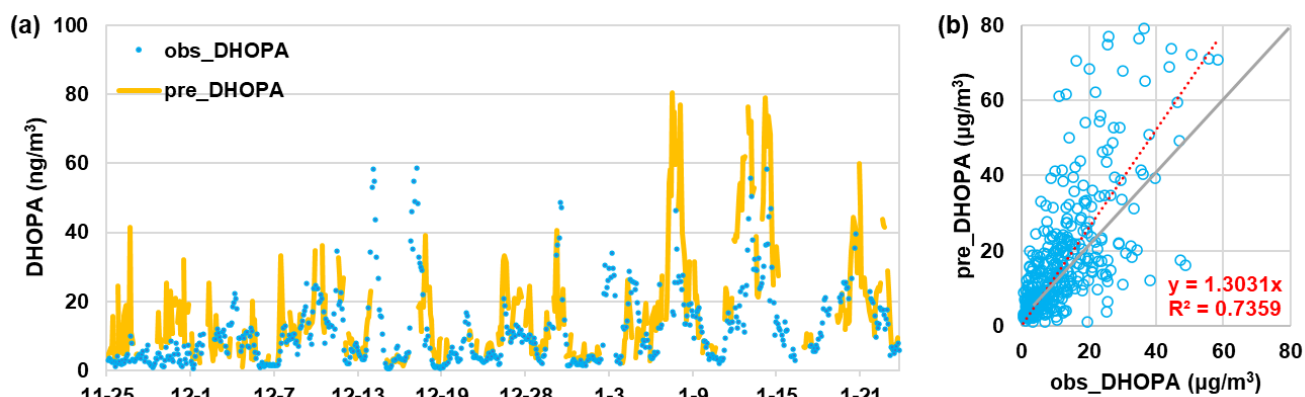


Figure S9. (a) Predicted and observed hourly concentrations of DHOPA during the campaign; (b) scatter plots of predicted and observed hourly DHOPA. Dashed red line is the linear fit line with slope forced to zero based on all hourly dataset and solid grey line is the 1:1 line.

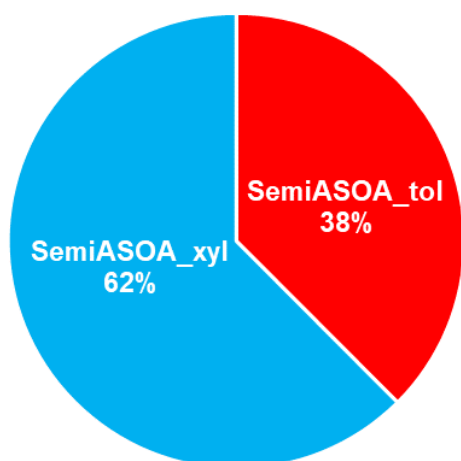


Figure S10. Predicted contributions to DHOPA from toluene and xylene pathways under high- NO_x conditions.

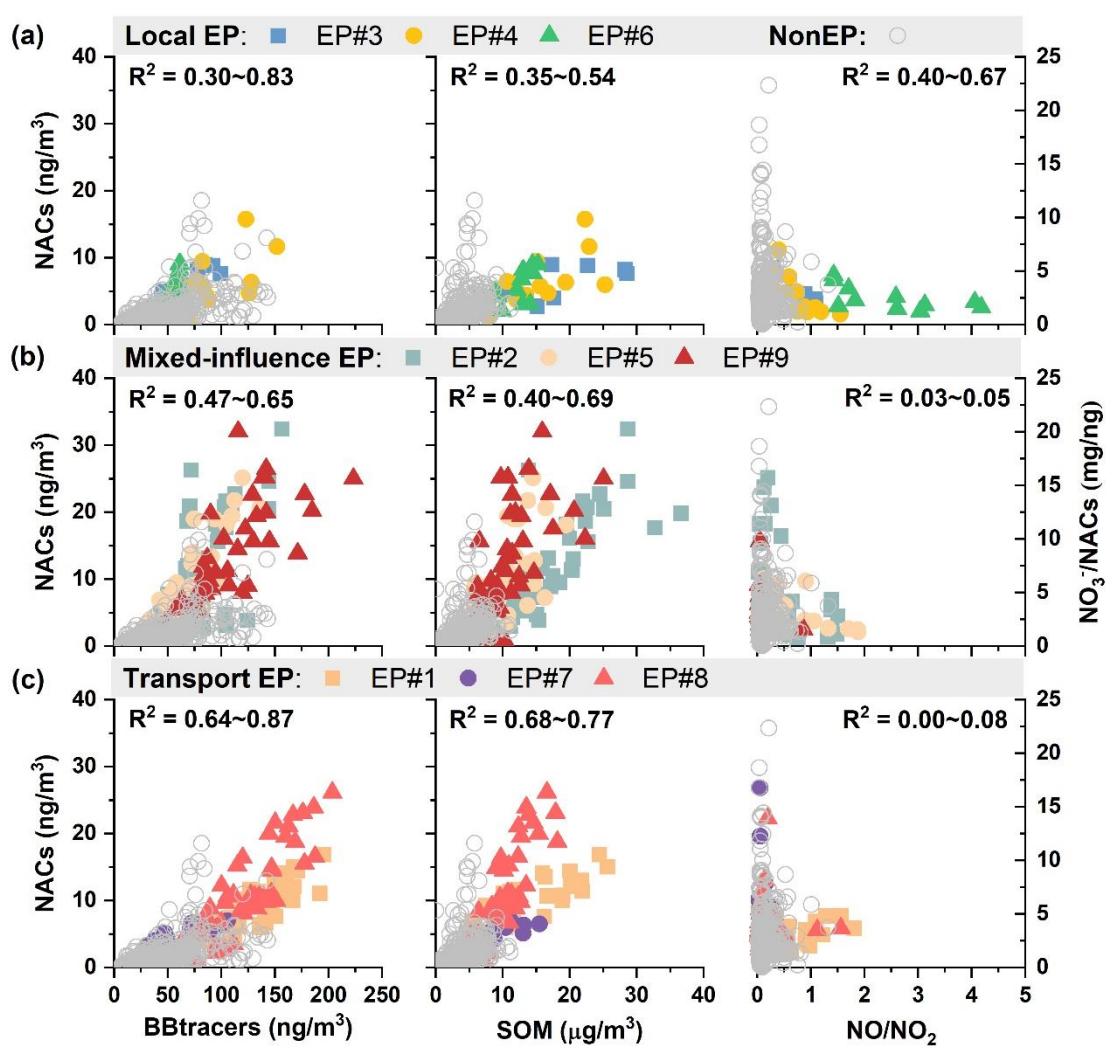


Figure S11. Correlations of NACs versus biomass burning tracers (BBtracers), SOM and nitrate to NACs ratios versus NO/NO_2 ratios during (a) local, (b) mixed-influence and (c) transport episodes.

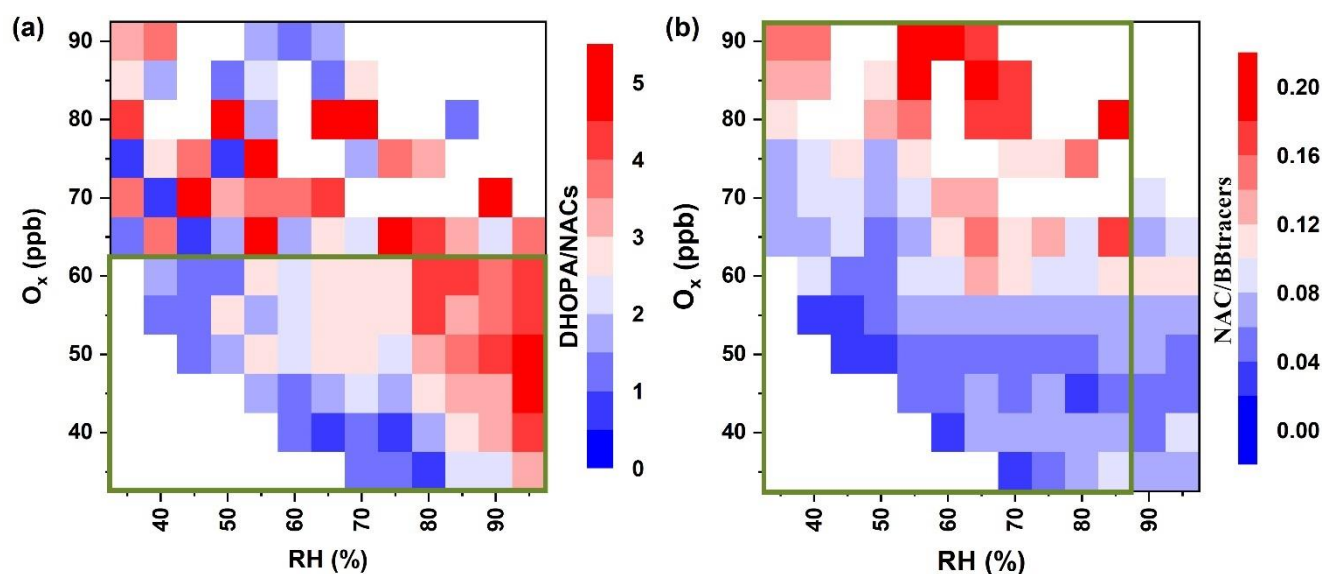


Figure S12. RH versus O_x dependence of the mass ratios of (a) DHOPA to NACs and (b) NACs to biomass burning tracers during the field campaign.

References

- Al-Naiema, I., Offenberg, J. H., Madler, C. J., Lewandowski, M., Kettler, J., Fang, T. and Stone, E. A.: Secondary organic aerosols from aromatic hydrocarbons and their contribution to fine particulate matter in Atlanta, Georgia, *Atmospheric environment* (1994), 223, 117227, 10.1016/j.atmosenv.2019.117227, 2020.
- Borbon, A., Gilman, J. B., Kuster, W. C., Grand, N., Chevaillier, S., Colomb, A., Dolgorouky, C., Gros, V., Lopez, M., Sarda-Esteve, R., Holloway, J., Stutz, J., Petetin, H., McKeen, S., Beekmann, M., Warneke, C., Parrish, D. D. and de Gouw, J., A.: Emission ratios of anthropogenic volatile organic compounds in northern mid-latitude megacities: Observations versus emission inventories in Los Angeles and Paris, *Journal of geophysical research. Atmospheres*, 118, 2041-2057, 10.1002/jgrd.50059, 2013.
- Bressi, M., Sciare, J., Gherzi, V., Mihalopoulos, N., Petit, J. -, Nicolas, J. B., Moukhtar, S., Rosso, A., Féron, A., Bonnaire, N., Poulakis, E. and Theodosi, C.: Sources and geographical origins of fine aerosols in Paris (France), *Atmospheric chemistry and physics*, 14, 8813-8839, 10.5194/acp-14-8813-2014, 2014.
- Gouw, J. A., Gilman, J. B., Kim, S. -, Alvarez, S. L., Dusanter, S., Graus, M., Griffith, S. M., Isaacman-VanWertz, G., Kuster, W. C., Lefer, B. L., Lerner, B. M., McDonald, B. C., Rappenglück, B., Roberts, J. M., Stevens, P. S., Stutz, J., Thalman, R., Veres, P. R., Volkamer, R., Warneke, C., Washenfelder, R. A. and Young, C. J.: Chemistry of Volatile Organic Compounds in the Los Angeles Basin: Formation of Oxygenated Compounds and Determination of Emission Ratios, *Journal of geophysical research. Atmospheres*, 123, 2298-2319, 10.1002/2017JD027976, 2018.
- Gao, Y., Wang, H., Zhang, X., Jing, S., Peng, Y., Qiao, L., Zhou, M., Huang, D. D., Wang, Q., Li, X., Li, L., Feng, J., Ma, Y. and Li, Y.: Estimating Secondary Organic Aerosol Production from Toluene Photochemistry in a Megacity of China, *Environ. Sci. Technol.*, 53, 8664-8671, 10.1021/acs.est.9b00651, 2019.
- Kleindienst, T. E., Jaoui, M., Lewandowski, M., Offenberg, J. H., Lewis, C. W., Bhawe, P. V. and Edney, E. O.: Estimates of the contributions of biogenic and anthropogenic hydrocarbons to secondary organic aerosol at a southeastern US location,

Atmospheric environment (1994), 41, 8288-8300, 10.1016/j.atmosenv.2007.06.045, 2007.

Waked, A., Favez, O., Alleman L, Y., Piot, C., Petit, J., Delaunay, T., Verlinden, E., GOLLY, B., Besombes, J. and Jaffrezo, J.: Source apportionment of PM₁₀ in a north-western Europe regional urban background site (Lens, France) using positive matrix factorization and including primary biogenic emissions, Atmospheric chemistry and physics, 14, 3325-3346, 10.5194/acp-14-3325-2014, 2014.

Yuan, B., Shao, M., de Gouw, J., Parrish, D. D., Lu, S., Wang, M., Zeng, L., Zhang, Q., Song, Y., Zhang, J. and Hu, M.: Volatile organic compounds (VOCs) in urban air: How chemistry affects the interpretation of positive matrix factorization (PMF) analysis, Journal of Geophysical Research: Atmospheres, 117, n/a, 10.1029/2012JD018236, 2012.

Zhang, J., He, X., Gao, Y., Zhu, S., Jing, S., Wang, H., Yu, J. Z. and Ying, Q.: Assessing Regional Model Predictions of Wintertime SOA from Aromatic Compounds and Monoterpenes with Precursor-specific Tracers, Aerosol and air quality research, 21, 210233, 10.4209/aaqr.210233, 2021a.

Zhu, Y., Yang, L., Kawamura, K., Chen, J., Ono, K., Wang, X., Xue, L. and Wang, W.: Contributions and source identification of biogenic and anthropogenic hydrocarbons to secondary organic aerosols at Mt. Tai in 2014, Environ. Pollut., 220, 863-872, 10.1016/j.envpol.2016.10.070, 2017.